Retro Rocket Motor Self-Penetrating Scheme for Heat Shield Exhaust Ports

Colleen Marrese-Reading, Josh St.Vaughn,
Jet Propulsion Laboratory
4800 Oak Grove Dr.
Pasadena, CA 91109
818-354-8179
Colleen.M.Marrese-Reading@jpl.nasa.gov

Peter Zell and Ken Hamm
NASA Ames Research Center
Mail Stop 230-2
Moffett Field, CA 94035
650-604-3690
Peter.T.Zell@nasa.gov

Jim Corliss and Steve Gayle
NASA Langley Research Center
Hampton, CA23681
757-864-7627
James.M.Corliss@nasa.gov

Rob Pain, Dan Rooney, Amadi Ramos, and Doug Lewis
ATK Tactical Propulsion and Controls
55 Thiokol Road
Elkton, MD 21921
410-392-1296
Robert.Pain@ATK.com

Joe Shepherd and Kazuaki Inaba
California Institute of Technology, Mail Code 105-50
1200 East California Blvd
Pasadena, CA 91125 USA
626-395-3283
Joseph.E.Shepherd@caltech.edu

Abstract—A preliminary scheme was developed for base-mounted solid-propellant retro rocket motors to self-penetrate the Orion Crew Module heat shield for configurations with the heat shield retained during landings on Earth. In this system the motors propel impactors into structural push plates, which in turn push through the heat shield ablator material. The push plates are sized such that the remaining port in the ablator material is large enough to provide adequate flow area for the motor exhaust plume. The push plate thickness is sized to assure structural integrity behind the ablative thermal protection material. The concept feasibility was demonstrated and the performance was characterized using a gas gun to launch representative impactors into heat shield targets with push plates. The tests were conducted using targets equipped with Fiberform® and PICA as the heat shield ablator material layer. The PICA penetration event times were estimated to be under 30 ms from the start of motor ignition. The mass of the system (not including motors) was estimated to be less than 2.3 kg (5 lbs) per motor. The configuration and demonstrations are discussed. [1,2]

TABLE OF CONTENTS

1. INTRODUCTION

Retro rockets were considered for the Orion Crew Module Earth landing system for nominal land landings (NLL) and contingency land landings (CLL) [1] early in the Orion architecture trade studies. However, the Orion Crew Module (CM) landing architecture currently requires the Earth return landings to be at a coastal Pacific Ocean landing site. In both NLL and CLL scenarios the motors would be base mounted behind the primary heat shield, and in each case the heat shield would be retained during landings to provide additional impact energy attenuation for the crew. In the CLL scenario, the retro rockets would fire in the last 0.5 s of descent with 155.8 kN (35,028 lb-f) of total thrust. The ignition altitude and thrust profile were derived to ensure that the touchdown vertical velocity would not exceed 4.6 m/s (15 ft/s) within a 95% probability. The baseline heat shield material for the Orion CM at the time this study was conducted was Phenolic Impregnated Carbon Ablator (PICA), which consists of a low density carbon fiber matrix substrate impregnated with a phenolic resin [2]. The initial form of the material as a carbon fiber matrix is Fiberform® that manufactured by Fiber Materials Incorporated. One of the primary challenges in implementing this system is perforating the ports in the PICA heat shield to provide clearance for the rocket motor exhaust, as shown in Figure 1, without adding undue risk to the primary function and

[1] 978-1-4244-2622-5/09/$25.00 ©2009 IEEE.
[2] IEEEAC paper #1449, Version 2, Updated Dec. 22, 2008

performance of the heat shield. An additional challenge is to ensure that the perforation event time is approximately 10x lower than the 0.5 s motor burn time to minimally impact the performance of the motor.

A scheme was developed for the motors to penetrate the heat shield to assess the feasibility, approximate the mass and retire some of the risk associated with the concept. In the selected approach the motors would provide the means to penetrate the heat shield and open the exhaust ports, rather than rely on a secondary system to perform this function. In this scheme the rocket motors propel impactors that would apply an impulsive and then static load on a structural push plate behind the heat shield, which would then punch out a push plate-sized port in the PICA. The penetration system is shown in Figure 2. The impactors would be blown out of the motor nozzle during start-up and accelerated by the force of the motor exhaust. Prior to proceeding with the impactor concept, the design team examined the possibility of relying only on the pressure and abrasiveness of the motors' exhaust products to penetrate the PICA. However, it was determined that the static thrust load of the smaller motors being considered in the retro rocket design would not be sufficient to open up large enough ports, and that the time required for the ports to open would be excessive relative to the motors' burn time. Seams and shape charges in the heat shield were also temporarily considered to assist in opening the exhaust ports, however, this approach was not selected due to concerns over the seams or shape charges failing during re-entry and imposing undesirable risk to the crew.

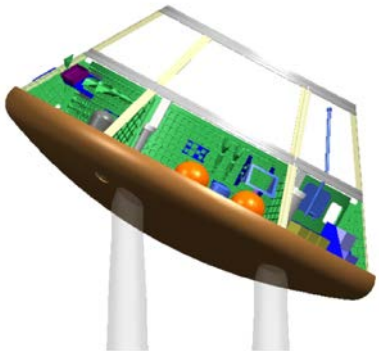

Figure 1 - Vertical retro rocket motors mounted behind the heat shield in Orion for the CLL.

A preliminary configuration for the impactor concept was developed and proof-of-concept demonstration tests were conducted to mitigate risk. The demonstration tests only simulated the initial impact load of the impactor hitting the push plate on the heat shield. The subsequent static motor exhaust load was not included in the testing because it is desirable to accomplish the penetration with just the initial impact load since this event time is expected to be much shorter than a process that relies on the motor static load to shear a port into the heat shield. The objective of the demonstration was to prove that the initial impact load would be sufficient to punch the desired port out of the heat shield. The additional static load from the motor should then further increase the load on the heat shield and improve the effectiveness of the process to further reduce the event time. The feasibility of the design was assessed for the CLL system because the lower motor thrust levels would provide lower energy impacts to the heat shield and therefore the greatest challenge. The design, mass and demonstration results are presented in this report.

2. CONFIGURATION

In the proposed approach to perforating the heat shield, impactors are blown out of the motor nozzles and into push plates which punch through the heat shield ablator material layer. The motor thrust levels are expected to be 22.3 kN (5,010 lb-f) for each of the two back motors and 55.6 kN (12,500 lb-f) for each of the two front motors for the current CLL retro rocket configuration. The heat shield penetration configuration is shown in Figure 2. It includes an impactor/penetrator in the motor nozzle, a structural support push plate behind the heat shield ablator material and possibly a stiffened cylinder to confine the exhaust if necessary.

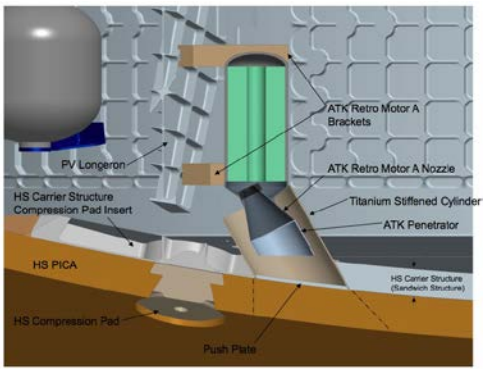

Figure 2 - The configuration of the penetration scheme with the retro rocket motor.

Titanium Stiffened Sleeve/Cylinder

The cylinder would consist of either a short sleeve in the heat shield carrier structure or a much longer structure extending between the heat shield and motor nozzle. The longer structure would be implemented if recirculation of the motor exhaust is problematic in the CM's aft bay or if exhaust pressure concentration is required for sufficient impactor acceleration. This cylinder would consist of a titanium sleeve and an additional or continuous titanium cylinder or an Ethylene Propylene Diene Monomer (EPDM) cylinder between the sleeve and nozzle to seal around the motor nozzle and the sleeve. If the cylinder is not required

to contain the exhaust, then only a sleeve will be employed on the inner diameter of the heat shield carrier structure for reinforcement to structurally compensate for the opening in the carrier structure. Structural analysis was conducted to identify the thickness of the sleeve required to prevent any increase in the carrier structure deflection with the opening. A finite element model was developed using a square sandwich plate that was simply supported around all of the edges with a width that was equivalent to the circumferential distance between longerons at the radius of the compression pads. The face sheets were modeled with shell elements (CQUAD4) and the core was modeled with solid elements (CHEXA). The applied load to the carrier structure in the analysis was 68.9 kPa (10 psi). In this configuration the sleeve thickness in the port will need to be 0.28 cm (0.11 in.) with a length of 6.1 cm (2.4 in.). The mass of a 20.3 cm (8 in.) diameter sleeve was estimated to be 0.72 kg (1.6 lbs) including the fasteners and braze mass.

Push Plate

The push plate provides structural support behind the heat shield to simulate the Ti-Ti (Ti plates and crushable Ti honeycomb structure) carrier structure. The push plate diameter should define the size and shape of the port in the heat shield. This diameter is expected to be no greater than 20.3 cm (8 in.) to accommodate all of the rocket motors being considered in the landing system designs. The push plate material will be Ti and the thickness will depend on the expected pressures, radius-of-curvature (ROC) of the heat shield and how it is supported. Structural analysis was conducted to identify the simply supported Ti plate thickness required to prevent de-bonding of the PICA from the carrier structure and/or structural failure of the PICA. The ROC of the heat shield considered in the analysis was 508 cm (200 in.). The results of the analysis indicated that the thickness of an 8 in. diameter titanium push plate would need to be 2.95 mm (0.116 in.) to accommodate nominal re-entry loads, or 4.34 mm (0.171 in.) to accommodate late ascent abort re-entry loads. The masses of these two plates would be 0.45 kg (1 lb) and 0.69 kg (1.53 lbs) respectively.

Impactor

The impactor would be ejected from the nozzle and accelerated by the motor exhaust pressure to impact the push plate and heat shield with enough energy to completely penetrate through the heat shield. The impactor will be released when the motor exhaust pressure load on the impactor exceeds the ultimate shear strength on the mating ring to the nozzle. The diameter of the circular impactor would be approximately 12.7 cm (5 in) to fit within the motors' nozzles and the material would be stainless steel for the mass to exceed the push plate mass. A hemispherical front end on the impactor is preferred for a more determinant single point impact against the push plate should the impactor rotate slightly before contact with the push plate.

A CFD model was developed at ATK using Fluent® to simulate the release and acceleration of the impactor to estimate its final velocity considering the motor thrust level, exhaust recirculation if uncontained, back pressure on the impactor and the impactor mass. Two simulations were conducted to consider the influence of impactor mass on final velocity. The two masses that were considered were for 0.33 kg (0.73 lb) for an aluminum (Al) impactor, and 1.02 kg (2.25 lb for a stainless steel (SS) impactor, both assuming the same volume. The impactor acceleration process was simulated for a 3,500 lb motor firing in 0.5 s because this motor was readily available should the program proceed into using actual rocket motors for demonstration tests. The simulation configuration and pressure distribution results are shown in Figure 3. The CFD analysis results for the pressure on the impactor and the impactor velocity for the Al and SS impactors are shown in Figure 4. The results showed that the pressure build-up on the opposite side of the impactor and recirculation in the aft bay reduces the acceleration force on the impactor. The final velocities for the impactors were 30 (SS) and 42 m/s (Al) and impact energies were 453 J (SS) and 284 J (Al). A motor thrust equivalent load behind the impactors would produce velocities of 48.2 m/s (SS) and 84.6 m/s (Al). Confining the motor exhaust with a sleeve will increase the final velocities of the impactors compared to the simulation results. The larger motors in the retro rocket configuration with higher thrust levels will also produce higher velocity impactors. Additional CFD analysis is required to consider the actual motor thrust levels and identify the expected impactor velocities for various impactor masses and exhaust confinement scenarios.

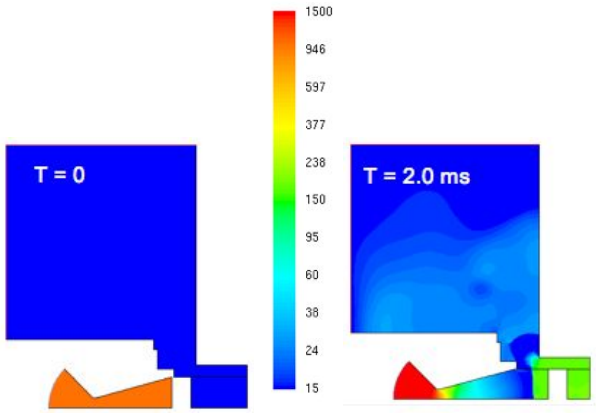

Figure 3 - The CFD simulation configuration and the pressure distribution at 0 sec and then at 2.0 ms.

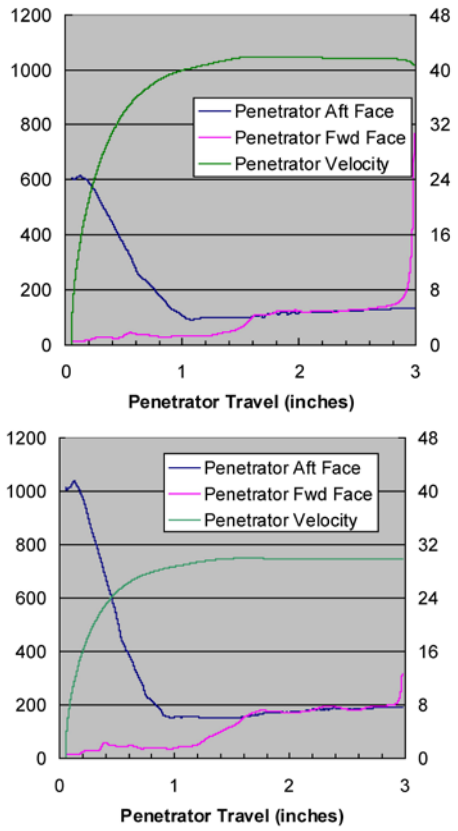

Figure 4 – The motor exhaust pressure (left axis) on the impactor and the impactor velocity (right axis) predicted in the CFD analysis for Al (left) and steel (right) impactors.

3. MASS

A preliminary mass for the system can be identified based on the preliminary estimates for the configuration elements. The mass of a titanium sleeve is expected to be 0.7 kg (1.6 lbs). The mass of the push plate is expected to be 0.7 kg (1.5 lbs) for late ascent abort, and 0.45 kg (1 lb) for a nominal re-entry scenario. The mass of the impactor is expected to be at least 0.6 kg (1.3 lbs) and could be as high as 0.9 kg (2 lbs.). Therefore, the upper limit on the total system mass is estimated to be 1.7 – 2.3 kg (3.8-5 lbs).

4. DEMONSTRATION

Preliminary demonstration tests were conducted to prove that the proposed motor self-penetrating heat shield scheme is feasible and to characterize its performance. The objectives of the tests were 1) to test the feasibility of the penetration scheme, 2) to identify the ballistic impact limit for the PICA and the penetration scheme if possible and 3) to quantify the ballistic impact event time. A ballistic impact is defined by complete penetration of the target and the ballistic limit is the minimum velocity that results in complete penetration for the specific projectile and target. [3] In the tests the impactors were accelerated up to representative velocities by a gas gun to impact push plates on heat shield targets to simulate and demonstrate the proposed penetration scheme. The tests were conducted at representative impact energies with Fiberform® and then PICA targets.

Test Facility

The ballistic impact tests were conducted in a gas gun facility at the California Institute of Technology (Caltech). This facility employs a vertical gas gun, a Phantom VII high speed video camera, a laser system for projectile velocity measurements and a high speed (2MHz) data acquisition system. The gas gun can launch 5 cm (2 in.) diameter projectiles at speeds up to 250 m/s. The gas gun and facility configurations are shown in Figure 5. The projectile is launched by activating a valve to switch from vacuum to pressurized air behind the impactor. An LK-G407 Keyence CCD laser displacement sensor was implemented for the PICA tests to measure the push plate displacement during the impact events. This system operates at 50 kHz with a 15.75 ±3.94 in. range (400 ±100 mm), ±0.05% accuracy and 0.08 mil (2 um) resolution.

Impactors

The impactors were constructed from aluminum to facilitate the gun operation and provide the desired mass. They have a hemispherical front end as shown in Figure 7. The mass of the hemispherical impactors used in the tests was 0.6 kg (1.3 lbs). They have a diameter of 50 mm (2 in.) and a length of 12.1 cm (4.8 in.). They have o-rings to provide a gas seal between the pressurized chamber and the barrel of the gun.

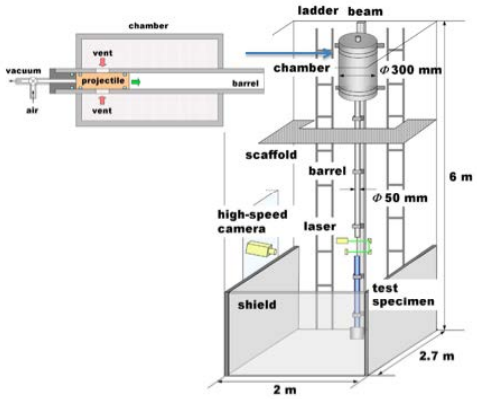

Figure 5 - The gas gun configuration and facility configuration depiction.

Figure 6 - Picture of the Caltech vertical gas gun.

Figure 7 - The hemispherical impactor.

Heat Shield Targets

The heat shield targets were constructed to simulate the heat shield and carrier structure with the push plates required in the penetration scheme. They were constructed from Fiberform® or PICA tiles, aluminum support plate frames and titanium push plates as shown in Figure 8. Aluminum support plates were bonded to the heat shield material with RTV 560. The first two targets in Tests 1 & 2 were constructed with 0.16 cm (1/16 in.) thick aluminum frames. In the following tests these Al plates were rigidized with 1.3 cm (0.5 in.) thick Al plates and epoxy between them. Tests 1-2 employed 0.16 cm (1/16 in.) thick push plates. Tests 3-8 employed 0.3 cm (1/8 in.) push plates. In tests 1-6 the Fiberform® and aluminum frames were bonded with RTV between them only. In tests 7-8 the PICA and Al frame were bonded with the Strain Isolation Pad (SIP) layer and RTV, as would be employed in flight.

Fiberform® targets were used in initial tests because they are much less expensive than PICA, more readily available and Fiberform® is a reasonable simulator for PICA during test development. Fiberform® is the initial state of PICA as the carbon fiber matrix before being impregnated with a phenolic resin to improve its thermal and structural properties. Undamaged Fiberform® is shown in Figure 9. Fiberform® is expected to be ~50% more brittle than PICA. Therefore the Fiberform® test results can be applied to estimate the ballistic impact energies required for the PICA targets.

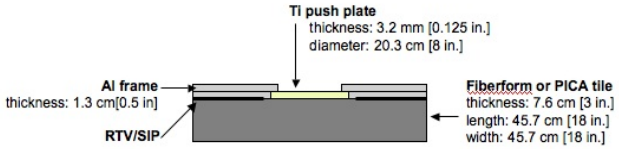

Figure 8 - The target configuration and materials.

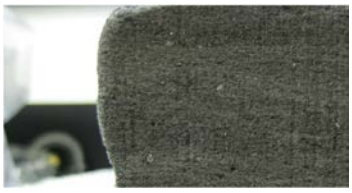

Figure 9 - The structure of the Fiberform® target.

Tests/Results

Three series of tests were conducted with Fiberform® and PICA targets. Fiberform® targets were tested in the first two series of tests and PICA was tested in the third series of tests. The conditions for each of the tests are presented in Table 1. The support plate deflected considerably in test series 1 under the impact loads, therefore much thicker plates were used in test series 2 & 3 to behave more similar to the rigid carrier structure that it was simulating. The gas gun was developed for much higher velocities than required in these tests. At the low velocities targeted, the impactor velocity was difficult to control. Therefore, the impactor velocities were typically higher than the target value, as shown in Table 1 as the velocity objective.

Both successful and unsuccessful penetration tests were conducted with the Fiberform® targets. The test facility is shown in Figure 10 with the targets installed. The impactor did not penetrate the target in Test 3 with a velocity of 20 m/s (65.6 ft/s). The high speed video showed that the impactor pushed the plate 1.27 cm (0.5 in.) into the Fiberform®, before it bounced off. The target was cross-sectioned after the test to examine the depth of the circumferential shear fracture in the Fiberform® around the push plate and any other fractures in it. Fractures were observed that originated from the back side of the target and propagated back towards the push plate partially through the target. Considering the impactor bounce height, the mass of the impactor and its initial energy, the energy imparted to the target could be identified. The initial energy of the impactor was 120 J. The kinetic energy after the impact was 0.72 J. The impact energy was not sufficient for target penetration.

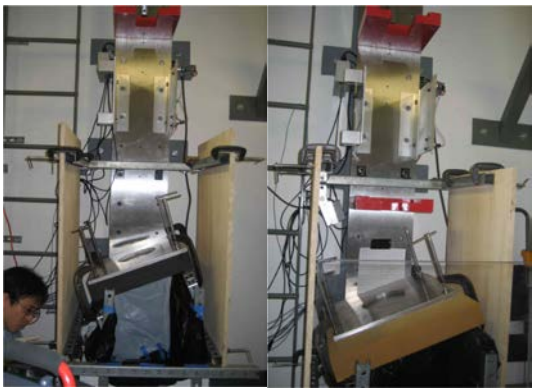

Figure 10 - The test configuration with Fiberform® (left) and PICA (right) targets installed at 22°

Penetration was demonstrated with the Fiberform® targets with impact energies in the range expected from the motors. The impactor velocities in these tests ranged from 34.7 m/s (114 ft/s) to 61.1 m/s (200 ft/s) in Tests 1, 2, 4, 5, and 6 at 0 and 22°. The minimal impact energy tested in Test Series 2 that produced penetration was 467 J at 39.3 m/s (128.9 ft/s) in Test 5. In this test the combination of plate deformation, inelastic collision and perforation energy was >407 J, as derived from the initial and final energy estimates. Test results shows that the higher impact energies produced larger diameter ports in the targets. Figure 11 shows pictures of the target after the impact in Test 5. The impactor completely passed through the target within 19.6 ms and the push plate passed through the target within less than 11 ms in this test. Figure 12 shows pictures of the target after Test 6. Circular plugs of material were pushed out of the targets in addition to many fragments that were blown out of the targets' back sides. The initial shapes of the ports are circular like the push plate and then open up towards the back surface where the material spalls out. The Fiberform® in the plug and the material in the target around it have a layered structure. Figure 12 also shows a reconstruction of the target with some of the material blown out of it, revealing the fracture pattern in it before the port was opened up in it.

Table 1 - Test conditions and results

Test #	Target Material	Impactor Mass	Push Plate Mass	Impactor Velocity *(Objective)*	Results
Test Series 1					
1	Fiberform®	0.59 kg [1.28 lbs]	0.23 kg [0.51 lb] (t= 1/16 in.)	61.1 m/s [200 ft/s] *(78 m/s [257 ft/s])*	SUCCESSFUL
2	Fiberform®	0.59 kg [1.28 lbs]	0.23 kg [0.51 lb] (t= 1/16 in.)	34.7 m/s [114 ft/s] *(30 m/s [96 ft/s])*	SUCCESSFUL
Test Series 2					
3	Fiberform®	0.6034 kg [1.327 lbs]	0.46 kg [1 lb] (t=1/8 in.)	20 m/s [65.6 ft/s] *(25 m/s [82.0 ft/s])*	NOT SUCCESSFUL - impactor pushed plate ~1.3 cm into the fiberform and then bounced
4	Fiberform®	0.6034 kg [1.327 lbs]	0.46 kg [1 lb] (t=1/8 in.)	48.1 m/s [157.8 ft/s] *(40 m/s [131.2 ft/s])*	SUCCESSFUL Time: ~9.8 ms
5	Fiberform®	0.6034 kg [1.327 lbs]	0.46 kg [1 lb] (t=1/8 in.)	39.3 m/s [128.9 ft/s] *(35 m/s [114.8 ft/s])*	SUCCESSFUL Time: ~10.7 ms
6	Fiberform®	0.6034 kg [1.327 lbs]	0.46 kg [1 lb] (t=1/8 in.)	41.7 m/s [136.8 ft/s] at 22° *(39.3 m/s [128.9 ft/s] at 22°)*	SUCCESSFUL
Test Series 3					
7	PICA	0.59 kg [1.28 lbs]	0.46 kg [1 lb] (t=1/8 in.)	62.2 m/s [204.1ft/s] at 22° *(56.5 m/s)*	SUCCESSFUL Time: ~7.7 ms Initial push plate velocity: ~21.8 m/s Final push plate velocity: ~8 m/s
8	PICA	0.59 kg [1.28 lbs]	0.46 kg [1 lb] (t=1/8 in.)	57.5 m/s [188.6 ft/s] at 22° *(48.6 m/s)*	SUCCESSFUL Time: ~16.5 ms Initial push plate velocity: ~16.2 m/s Final push plate velocity: ~3.5 m/s

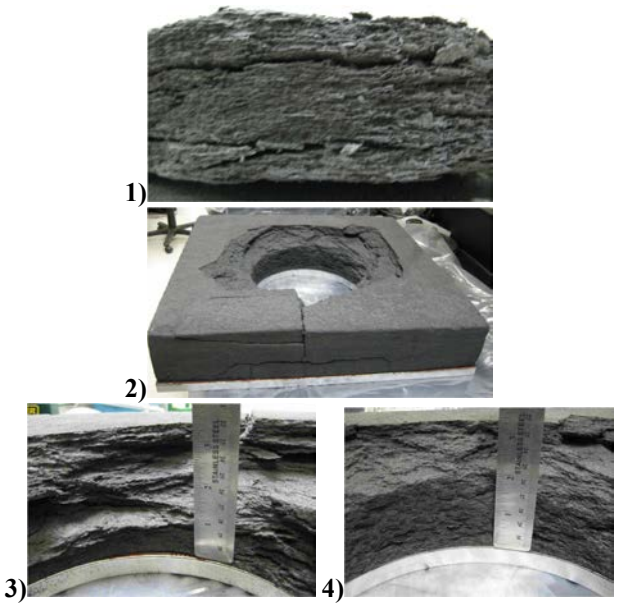

Figure 11 - Fiberform® target after impact during test 5: 1) the plug of Fiberform® pushed out of the target 2) the port created from the impact on the push plate 3&4) the shape of the Fiberform® at the wall of the port.

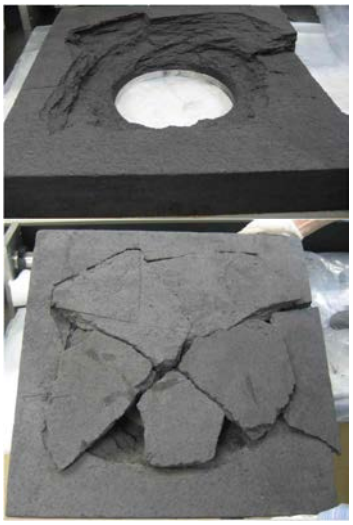

Figure 12 - The Fiberform® target after impact during test 6: 1) the port in the target created by the impact on the push plate, 2) the target reconstructed from the fragments of Fiberform® blown out from the impact.

Two impact tests were conducted with the PICA targets. The impactor energy in these experiments was more than 100% higher than the minimum energy that produced complete push plate penetration for the Fiberform® targets. PICA is considered to be **50%** less brittle than Fiberform® and has a density that is 75% higher. With only 2 available test targets, the high velocities were targeted to ensure success. Figure 13 shows the target after the impact and the reconstructed target that reveals the fracture pattern in the target. Figure 14 shows two frames from the video of the impact event that span about 0.8 ms. First contact is being made in the first frame and the second frame is the last frame that shows the impactor penetrating into the target without any bending deformation of the target. Figure 15 shows frames from the video during the impact with bending deformation in the target and final blow out of the port. Figure 16 shows the push plate displacement during the impact event. The push plate is displaced 1.8 cm (0.71 in) into the target during the first 0.8 ms with the plate velocity of 21.8 m/s (71.5 ft/s). At approximately 0.8 ms the video shows that the target begins to bend and fractures propagate and the target material gets blown out of it. The push plate displacement measurements show that the push plate travels through it at 8 m/s (26.2 ft/s) during this phase. The time for this impact event was estimated to be 7.68 ms from first contact to the push plate clearing the heat shield.

Figure 13 - Test 7 PICA target impact damage and target reconstructed from the fragments.

Figure 14 - Impactor penetrating into the target in Test 7 with with no deformation of outer surface in the first 0.8 ms.

A second ballistic impact was demonstrated with a PICA target in Test 8 with an impactor velocity of 57.5 m/s (188.6 ft/s) and impact angle of 22° at a normal velocity component of 53.3 m/s (174.9 ft/s). Figure 17 shows the target after the impact and the reconstructed target that reveals the fracture pattern in the target. Figure 17 also shows the layered PICA plug that was pushed out of the target. The same layering

structure was observed around the plug. The Fiberform® target also exhibited the layered structure around the impact site. The videos revealed the same process and time scales as shown for Test 7 in Figures 13 and 14. The push plate displacement data shown in Figure 15 confirms the same process and event times with a comparison of the data from Tests 7 and 8. In test 8 the impactor slipped at contact, flipped, and then rotated over the target. Therefore, it did not go through the target on the push plate as it did in Test 7. In this test the push plate was displaced ~ 1.4 cm (0.55 in) into the target during the first 0.8 ms with the plate velocity of 16.2 m/s (53.2 ft/s). At approximately 0.8 ms the video shows that the target begins to bend and fractures propagate and then the target material fractures. The push plate displacement measurements show that the push plate significantly slows down and then travels through the target at 3.5 m/s (11.5 ft/s) during this phase. The very low velocity phase may correspond to the impactor slipping sideways and temporarily removing the load from the plate before making contact again and pushing out the plate at 3.5 m/s (11.5 ft/s). The time for the push plate to clear the heat shield after the initial impact was 16.5 ms during test 8.

Figure 15 - Penetration event in Test 7 with bending deformation, tensile fiber breakage, tensile crack propagation and material spallation.

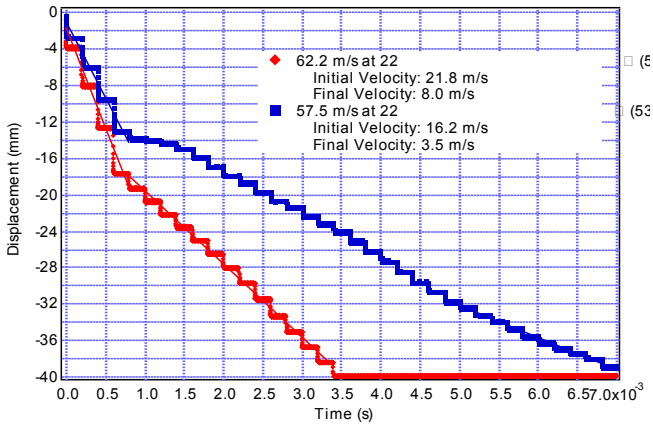

Figure 16 - Push plate displacement during the impact in Test 7 (red) & 8 (blue).

Figure 17 - PICA target impact damage during Test 8.

5. Discussion of Test Results

During the penetration event, the impactor kinetic energy is absorbed by the target during the inelastic collision with the push plate and in several destructive mechanisms that can lead to the perforation of the target when sufficient energy is applied. These mechanisms have been characterized for thick composites and our observations are consistent with composite failure processes under impact loads. [3,4] The mechanisms include plate deformation, target shear plugging, compression, friction, bulge formation, matrix cracking and spallation. The post-test target inspections, videos, and push plate displacement measurements suggest the following sequence of events during the impact as illustrated in Figure 18:

1) Impactor projectile undergoes inelastic collision with the push plate and target absorbing most of the impact energy to bring the impactor and pushplate to a common velocity and deform the plate.
2) Compression and shear waves are launched through target from impact.
3) Concentrated shear stress around the push plate creates a circumferential fracture that is driven into the target while the push plate energy is sufficient, creating a punching shear failure and a plug of target material.
4) Compression waves reach outer surface and cause it to bulge out.

5) Bulging initiates the tensile failure of the fibers on the backside of the target which introduces matrix cracks from the outer surface and starts a pattern of tensile matrix cracks that propagate back towards the impact site. These cracks induce significant separation between the layers in the target material. Bulge formation stops if the plate velocity reaches zero in the target.
6) Compression waves created from impact are reflected off of the opposite surface as tension waves. Fibrous material gets compressed by compression waves which breaks the cross fibers and then gets pulled apart into layers by the tension waves.
7) Large fragments of material are generated by matrix cracks and are then pushed out of the target by the plate. Final failure takes place because of the induced tensile stress along the radial direction.

An upper limit on the change in kinetic energy of the impactor, push plate and target can be estimated assuming that the impactor and push plate move forward together at the same velocity after the impact and that the PICA plug moves at the final push plate velocity. The mass of the PICA plug was estimated assuming an 8 in. diameter cylindrical port. This PICA velocity and mass underestimate will result in a low PICA kinetic energy estimate and high kinetic energy change estimate and therefore, a high estimate for the perforation energy. The change in kinetic energy was estimated to be ~ < 943 J in Test 7. The Fiberform® tests revealed that the port size increased with impact energy, and therefore the perforation energy estimate will also be high if the impact energy exceeded the ballistic impact limit. In this test, the initial inelastic impact collision consumed ~747 J. The perforation energy was estimated to be only ~196 J.

The required ballistic impact energy for the PICA target and penetration scheme was predicted from the Fiberform® test results. The impactor energy required for a ballistic impact in the configuration tested with a Fiberform® target was estimated to be ~407 J. The ballistic impact limit for PICA was expected to be 610 J (if 50% more energy is needed for PICA relative to Fiberform®) or 814 J (if 100% more energy is required). The PICA is understood to be 50% less brittle than Fiberform® with a density that is 75% higher. The target impact energy for the PICA tests was ~100% more than the ballistic impact energy required for the Fiberform®. A ballistic impact was demonstrated for the 3 in. thick PICA target with 0.6 kg impactor with a velocity of 57 m/s (188.6 ft/s), at 22°, (53.3 m/s normal to the plate) with a 0.46 kg (1 lb) push plate in Test 8. The normal impact energy in this test was 852 J. The energy dissipated by the target was estimated to be < 842 J. This amount of energy may be higher than necessary for the penetration because higher energy impacts create larger ports and therefore absorb more energy. Over 80% of the energy was dissipated by the initial inelastic collision between the impactor and plate. The impact energy limit for the penetration was not identified in these PICA impact tests, however it is less than the demonstrated level of 852 J. The PICA perforation energies in Test 7 & 8 were estimated to be less than 200 J for the configuration tested.

The pressure wave propagation speed can be estimated from the video data. The video shows that the bulge forms at 1.06 ms and 3 in. from the impact. These data suggest that the pressure wave propagation speed is ~72 m/s.

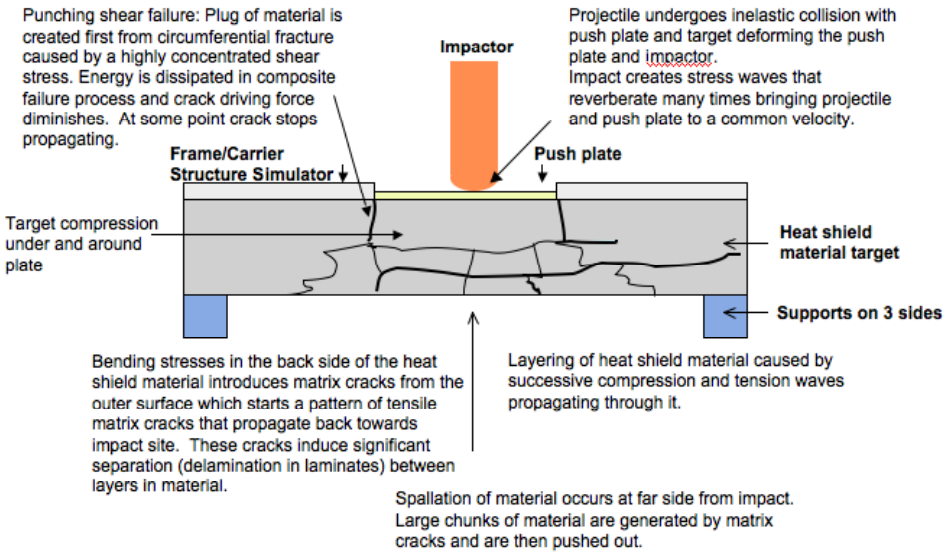

Figure 18 - Key elements of the failure process of the composite fiber targets under impact loads.

6. SUMMARY AND CONCLUSIONS

A retro rocket motor self-penetrating scheme for PICA heat shield exhaust ports was designed and conceptually demonstrated. This heat shield architecture option provides adequate structural support behind the ablative thermal protection material without the need for external seams or gaps. This approach has the potential to enable a retro-rocket-based vehicle landing impact attenuation solution without a corresponding increase in the risk of heat shield burn through during the critical atmospheric entry phase. CFD analysis was conducted to predict impactor acceleration by potential motors. Impactors were launched into push plates on PICA targets to characterize the effectiveness of the impactor and push plate configuration in punching out the desired port in the heat shield. The concept was successfully demonstrated with 2 ballistic impacts (complete penetration) with PICA targets with representative impactor velocities, system element masses and materials.

In addition to demonstrating the concept feasibility, critical performance elements of the system were characterized. The PICA penetration event times were measured to be less than 20 ms. Impactor acceleration times were predicted to be < 10 ms. Therefore, the penetration event times are expected to be less than 30 ms. Velocities of the impactors and push plates were measured to identify impactor and plate energies and velocities that enable complete penetration with 7.6 cm (3 in.) PICA targets. The 20.3 cm (8 in.) diameter plate impacting the PICA at 16.2 m/s (53.1 ft/s) with a mass of 0.45 kg (1 lb) had sufficient energy for a ballistic impact. The event time scales suggest that pressure waves are propagating through the PICA at ~ 72 m/s (236 ft/s). The force estimates suggest that the impact loading on the PICA from an 20.3 cm (8 in.) plate that is sufficient for penetration is less than 6.7 kN (1518 lb-f) and that the impact shear strength is less than 206.8 kPa (30 psi).

The preliminary demonstration tests proved that the impact force from the impactor alone should be sufficient to open up motor exhaust ports in the heat shield within 30 milliseconds for the configuration tested. The additional static load from the motors is expected to accelerate the process and enable lower impact loads for successful penetrations. Additional tests should be conducted to identify the lower limits.

The penetration scheme should be tested with AVCOAT heat shield targets to determine if the concept is also feasible with that heat shield material if there is interest in this architecture.

ACKNOWLEDGEMENTS

The research described in this paper was carried out at the Jet Propulsion Laboratory, California Institute of Technology, under a contract with the National Aeronautics and Space Administration. The authors would like to thank Chris Johnson (NASA JSC), the CEV LS ADP, CEV TPS ADP and George Chen (JPL) for support for the project. The authors would also like to thank Al Owens for fabrication of several impactors and help assembling the targets.

REFERENCES

[1] C.J. Johnson, R.A. Hixon, R. A., "Orion Vehicle Descent, Landing, and Recovery System Level Trades, AIAA 2008-7745, AIAA Space 2008 Conference and Exposition, Sept. 9-11, 2008.

[2] Y.K. Chen, D Paragas, and L. Kobayashi, "Phenolic Impregnated Carbon Ablators (PICA) as Thermal Protection Systems for Discovery Missions," NASA TM-110440, April 1997.

[3] *Serge Abrate, Impact on Composite Structures*, Cambridge University Press, 1998.

[4] N.K. Naik and A.V. Doshi, "Ballistic Impact Behavior of Thick Composites: Analytical Formulation," AIAA Journal, Vol. 43, No.7, July 2005

BIOGRAPHY

Colleen Marrese-Reading *is a Senior Member of the Technical Staff in the Propulsion and Materials Engineering Section at the Jet Propulsion Laboratory. She has been working at JPL for over 13 years on the development of advanced propulsion systems. She led the last phase of the retro rocket landing system trade study for the Orion spacecraft. She received her B.S in Engineering Physics and M.S. and Ph.D. in Aerospace Engineering from the University of Michigan with two semesters at the Moscow Aviation Institute in Russia.*

Joshua St. Vaughn *is the Group Supervisor of the Mechanical Systems and EDL Group in JPL's Spacecraft Mechanical Engineering Section. He received his B.S. and M.S. in Mechanical Engineering from The Massachusetts Institute of Technology in 1993. He has spent over five years at the Jet Propulsion Laboratory. His experience includes mechanical system engineering roles on Mars Pathfinder, Champollion, and Micro-Spacecraft.*

James M. Corliss *has extensive experience as a project manager, systems engineer, and technical team leader for a variety of NASA aerospace and aeronautical projects. Currently, Mr. Corliss is serving as the Principal Engineer for the Orion Landing System Advanced Development Project (ADP), and recently served as the aerodynamic testing lead for Earth return capsules, the Technology Development Manager for the Mars Sample Return Earth Entry Vehicle, and the re-entry vehicle Team Leader for*

NASA's Office of Biological and Physical Research Free Flyer initiative.

Pete Zell *recently served as the Deputy Project Manager of the Orion Heat Shield Thermal Protection System Advanced Development Project. He has experience as a project manager, systems engineer, and test engineer for a variety of NASA aeronautics and space projects over the past 23 years. He received his B.S. and M.S. in aerospace engineering from California Polytechnic State University in San Luis Obispo.*

Ken Hamm

Steve Gayle

Rob Pain *has over 20 years experience in the solid rocket motor (SRM) industry. Currently program manager (PM) for NASA Langley Propulsive Landing Systems for Earth Entry Capsules, Rob is also PM for the Air Force Research Laboratory's Multimode Propulsion program, which is developing an innovative spacecraft propulsion technology. Rob also ran the SOFTLAND program for the Jet Propulsion Laboratory, which successfully demonstrated a controllable solid gas generator within a full 6DoF simulation for a Mars descent and entry vehicle.*

Dan Rooney *is a Preliminary Design Engineer in the Advanced Systems and Technologies group at ATK. He received his B.S. in Aerospace Engineering from St. Louis University and M.S. in Aerospace Engineering from the University of Tennessee Space Institute. He has been at ATK for three year focusing on preliminary design. Prior experience include solid rocket motor and gas generator design for numerous types of applications including air bag inflation, hypersonic motor ignition, munitions range extension, controllable solid propulsion systems, and attitude control systems.*

Amadi A. Ramos *is a senior engineer in the Upper Stages, Ordnance, and Controls Group at ATK. He is a candidate for an M.S. in Mechanical Engineering from Villanova University (May 2009). He has spent over 10 years in the aerospace and defense industry. His experience includes design engineering roles for Lunar Landers, Solid Flexstage for Extraterrestrial Landers, ATK launch Vehicle, a motor for hot gas testing of divert and attitude control systems, gas generator igniter to ignite the RS-68 bi-propellant liquid rocket booster engine for EELV, penetrator for heat shield blow thru of re-entry vehicle, and various ordnance programs.*

Doug Lewis

Joe Shepherd *is the CJ "Kelly" Johnson Professor of Aeronautics and Professor of Mechanical Engineering at the California Institute of Technology. He teaches and does research on fluid dynamics, structural mechanics, and propulsion.*

Kazuaki Inaba *is a postdoctoral scholar in Aeronautics at the California Institute of Technology. He received his B.S. and M.S. in Mechanical Engineering and Ph.D in Open and Environmental Systems from Keio University in 2005. After that he worked as an assistant professor of Mechanical Engineering in Tokyo University of Science, and he has spent two years at California Institute of Technology. His experience includes numerical simulations of detonation and pulse detonation engine interactions with turbine system, and experiments on fluid-structure interaction for marine structures.*